Transient characteristics of organic light-emitting diodes with efficient energy transfer in emitting material

Takeshi Fukuda[*,a], Bin Wei[b], Musubu Ichikawa[c], Yoshio Taniguchi[c]

[a]*Department of Functional Materials Science, Saitama University, 255 Shimo-Ohkubo, Sakura-ku, Saitama-shi, Saitama 338-8570, Japan*
[b]*Key Laboratory of Advanced Display and System Applications, Ministry of Education, Shanghai University, P.O.B. 143, 149 Yanchang Road, Shanghai 200072, P.R.China*
[c]*Faculty of Textile Science and Technology, Shinshu University, 3-15-1 Tokida, Ueda, Nagano 386-8567, Japan*

Abstract

We have investigated the combination effect of host-guest materials in an emitting layer on the transient property of an organic light-emitting diode (OLED). We found that an efficient energy transfer owing to the large overlap between the photoluminescence spectrum of host material and the absorption spectrum of guest material was important factor to improve the response speed of the OLED. As a result, the rise time of optical response was mainly affected by the combination of host-guest materials, and it increased using the optimal guest material, 1,4-bis[2-[4-*N*,*N*-di(*p*-tolyl)amino]phenyl]vinyl]benzene (DSB). A maximum -3 dB cutoff frequency of 15.8 MHz was achieved for an OLED with DSB as a guest material.

Key words: Organic light-emitting diode, Transient characteristics, Energy transfer, Host-guest material

1. Introduction

Organic light-emitting diodes (OLEDs) have attracted great interest for flat-panel display and lighting applications owing to their possibility of printable devices with a low fabrication cost [1, 2]. The high external quantum efficiency was achieved using novel organic emitting materials with the high

---

[*]Corresponding author. Tel.: +81-48-858-3526; fax: +81-48-858-3526.
Email address: fukuda@fms.saitama-u.ac.jp (Takeshi Fukuda)

internal quantum efficiency [3], the improvement in carrier balance in an emitting layer (EML) [4], and the efficient carrier injection from a metal cathode to an adjacent organic layer [5, 6]. In addition, the efficient carrier recombination in an EML is necessary to improve the luminescence efficiency, and the combination of host-guest materials is a one of the most important technique to avoid the concentration quenching, resulting in the realization of high device performance [7, 8, 9].

Promising results have been obtained indicating a potential application of OLEDs as light sources for optical communication systems owing to their fast electro-optical conversion speed [10, 11]. The merits of an organic light source are their large emitting area, flexibility, and low fabrication cost. In particular, a large emitting area, which realizes easy alignment between an organic light source and an organic photo diode, is difficult to be achieved utilizing inorganic materials. However, the electro-optical conversion speed of an OLED is lower than that of a conventional semiconductor light source, and the low response speed limits their application to optical communications.

A transient characteristic of an OLED is determined by combining various elementary electrochemical processes, including charge-carrier injection into organic layers from two electrodes (transparent anode and metal cathode), charge-carrier transportation in organic layers, buildup of space charges, formation of an excited state, and radiation decay from an excited state. Until now, several factors to affect transient properties of OLEDs have been already investigated, such as the capacitance determined by device area [12, 13], the fluorescence lifetime of light-emitting materials [14], the energy gap at the metal-organic interface [15], and the carrier mobility of electron/hole transport materials [16, 17, 18]. The reported -3 dB cutoff frequency was approximately 25 MHz with a small circular area of 300 μm diameter at a high applied voltage of 15 V [19]. However, the response speed is not high enough to transport high resolution movie file at the short time, and the further improvement in the response speed has been required for the practical application.

In this paper, we investigated the combination of host-guest materials in an EML to understand the carrier dynamics in stacked organic multilayer structure. The transient characteristic of optical response was estimated while applying pulse and sine wave voltages. We used three guest materials, 1,4-bis[2-[4-N,N-di(p-tolyl)amino]phenyl]vinyl]benzene (DSB), 4,4-bis(2,2-ditolylvinyl)biphenyl (DPVBi), and 4,4'-(bis(9-ethyl-3-carbazovinylene)-1,1'-biphenyl (BCzVBi), respectively.

2

2. Experimental

To ingestive the transient property of OLEDs with different combinations of host-guest materials, we fabricated three devices, referred as devices A (DSB), B (DPBVi), and C (BCzBVi). The cross sectional view of these devices are described in Fig. 1. At first, an indium tin oxide (ITO) anode with the thickness of 150 nm was sputtered on the top of the glass substrate, and the ITO-coated glass substrate was cleaned in deionized water, detergent, and isopropyl alcohol sequentially under ultrasonic waves. Next, the prepared glass substrate was treated with oxygen plasma for 5 min. Finally, organic layers and the MgAg (9:1 w/w)/Ag cathode were thermal evaporated at a base pressure of below 5.0×10^{-6} Torr. Each organic layer consisted of 4,4'-bis[N-(1-napthyl)-N-phenyl-amino]-biphenyl (α-NPD) as a hole transport layer, bathocuproine (BCP) as a hole block layer, and tris(8-hydroxyquinoline)aluminum (Alq$_3$) as an electron transport layer, respectively. Three organic emitting materials were choosed as DSB (device A), DPVBi (device B), and BCzVBi (device C) doped with 4, 4'-bis(9-dicarbazolyl)-2, 2'-biphenyl (CBP) at 0.5 wt.%, respectively. We estimated the concentration of host-guest materials by the evaporation rate of each material. The device structure was α-NPD 40 nm/EML 20 nm/BCP 10 nm/Alq$_3$ 20 nm/LiF 0.4 nm/MgAg 100 nm/Ag 50 nm. Emitting areas of all the devices were fixed at 1 mm^2.

We measured photoluminescence (PL) and absorption spectra of organic neat films using a spectrofluorometer (JASCO, FP-750) and a spectrometer (Hitachi, U3200), respectively. In addition, current density-voltage (J-V) and current efficiency-current density characteristics of devices were obtained using an OLED luminance efficiency measurement system (Precise Gauges, EL1003).

Rise and decay times of output electroluminescence (EL) intensity were measured while applying a pulse voltage with width of 1 μs to investigate the transient property. The bias and pulse voltages were applied to the device using a function generator (Agilent, HP81110A) and a DC power supply (ISO-TECH, IPS-3610D), respectively. Then, generated light was received using an avalanche photo diode (APD), and a time-resolved output power was measured with an oscilloscope (Yokogawa Electric, DL-1740). The rise and decay times were defined as the times required for the optical response to change from 10 to 90 % of the maximum EL intensity. The cutoff frequency of experimental setup was over 500 MHz, and the time constant of experimental

setup had less influence on the optical waveform of the OLED.

We also measured the EL intensity as a function of the frequency of an applied sine wave voltage. The sine wave and bias voltages were applied to OLEDs using a programmable FM/AM standard signal generator (KEN-WOOD, SG-7200) and a DC power supply, respectively. The output EL intensity was observed using an APD and an oscilloscope. The frequency dependence of EL intensity was measured by changing the frequency of the sine wave voltage from 100 kHz to 10 MHz.

3. Results and discussion

Figure 2 shows absorption coefficients of neat thin films of guest materials (DSB, DPVBi, and BCzVBi) and the PL spectrum of the CBP film, which was used as the host material in the EML. The peak wavelength of PL spectrum of CBP was 411 nm, and the PL intensity rapidly decreased in both shorter and longer wavelengths. The guest material had peculiar absorption band at the violet wavelength region. The peak wavelengths of absorption spectra of DSB, DPVBi, and BCzVBi were 418, 354, and 372 nm, respectively. Based on previous researches, the energy transfer efficiency of dye-doped OLEDs depends on the overlap integral of the emission spectrum of a host material and the absorption spectrum of a guest material. [20, 21]. The measured spectral overlap was different from each combination, and the largest value was achieved using DSB as a guest material. Therefore, efficient Förster energy transfer from the host material to the guest material is considered to be realized in the case of DSB doped CBP.

J-V characteristics of devices A (DSB), B (DPVBi), and C (BCzVBi) are shown in Fig. 3(a). Almost the same trends were obtained for all the devices because of the same device structure, such as thicknesses and energy levels of organic layer expect for the guest material. Figure 3(b) shows current efficiency-current density characteristics of three devices. As shown in Fig. 3(b), the OLED with DSB exhibited higher current efficiency (7.3 cd/A at the current density of 1 mA/cm^2) than other devices (0.9 and 1.5 cd/A at 1 mA/cm^2 for devices B (DPVBi) and C (BCzVBi). This tendency indicates that efficient energy transfer from the host material to the guest material causes the lower energy loss, resulting in the high current efficiency [8]. The current efficiency of all the devices decreased with increasing the current density owing to the low carrier recombination probability at the high electric

4

field. The maximum luminance of devices A (DSB), B (DPVBi), and C (BCzVBi) were 48690, 5613, and 18190 cd/m^2 at 10 V, respectively.

Figures 4(a) and (b) show rise and decay times of optical response while applying the pulse voltage. The bias voltage was fixed at 6 V and the pulse voltage was ranged from 5 to 10 V. In the cases of all the devices, both rise and decay times decreases with increasing the pulse voltage. When an electric field is applied across the device, holes and electrons are injected into an organic layer from the ITO anode and the MgAg cathode, respectively. Then, the injected carriers transport to the EML, resulting in the generation of light. Generally, the carrier mobility of organic material is lower than that of semiconductor materials [16], and the low carrier mobility limits the response speed of OLEDs [18]. The carrier mobility of organic materials increases with increasing the applied electric field in general [16]. Therefore, the higher carrier mobility at the high applied voltage causes the reduction of the carrier transport time from electrode to the EML [22]. As a result, both rise and decay times of optical response decreased with the increase of the applied voltage, as shown in Fig. 4.

The rise time of devices A (DSB), B (DPVBi), and C (BCzVBi) were 58, 345, and 257 ns at the pulse voltage of 5 V, respectively. Since the pulse width of applied voltage was 1 mus, the optical response was enough to saturate before turning off the voltage. As shown in Fig. 4, these values were larger than the decay time of all the devices. The large capacitance of emitting area limits the response speed of OLEDs owing to the large emitting area and the thinness of organic layers compared to semiconductor emitting devices [12, 13]. However the capacitance affects the both rise and decay times, and the capacitance of organic layers are almost same for all the devices. Therefore, we can conclude that the rise time of optical response is primarily associated with the carrier dynamics between the applying voltage and the generation of light. Furthermore, the fluorescence lifetime of DSB:CBP, DPVBi:CBP, and BCzVBi:CBP neat films at the concentration of 0.5 wt.% were 1.4, 1.6, and 0.8 ns, respectively. These values were estimated time-resolved PL intensity using a femtosecond pulse laser with the center wavelength of 390 nm and a streak camera. Such short fluorescence lifetimes were assumed to give little effect on response speed of devices [14].

The highest orbital molecular orbital (HOMO)/the lowest unoccupied molecular orbital (LUMO) levels of DSB, DPVBi, and BCzVBi were 3.1/5.5, 3.0/5.9, and 3.0/6.1 eV, respectively. In addition, the HOMO/LUMO levels of CBP were 2.4/6.0 eV. The high energy gap between the host material

and the guest material is considered to cause the reduction of the carrier transportation time from the host material to the guest material. However, the energy gap between DSB and CBP was higher than those of DPVBi and BCzVBi even though the rise time of optical response of the devices A (DSB) was shorter than those of devices B (DPVBi) and C (BCzVBi). Therefore, the experimental result in Fig. 4 cannot be explained the trap mechanism. One possible explanation of these experimental results in Figs. 2 and 4 is the host-guest energy transfer using Förster formalism. The holes and electrons are injected from the ITO anode and MgAg cathode to the CBP sites, respectively, and then excitons are formed. The excitonic energy is transferred to the guest sites, DSB, DPVBi, or BCzVBi for devices A, B, and C, respectively [21]. The efficiency of energy transfer relates with the overlap integral of the PL spectrum of the host material and the absorption spectrum of the guest material, and the large overlap integral is necessary for the efficient carrier recombination in the EML. Therefore, these experimental results in Figs. 2 and 4 confirm the hypothesis that the efficient energy transfer is useful to improve the response speed of OLEDs.

The frequency dependence of normalized EL intensity is shown in Fig. 5. The amplitude of sine wave voltage and the bias voltage were 7 and 5 V, respectively. Since the rise time of optical response of device A is fastest for all the devices, as shown in Fig. 4, the EL intensity of a high frequency region of device A is higher than those of other devices. The -3 dB cutoff frequency (f_c) is described as [23]

$$A = \frac{A_0}{1 + \frac{f}{f_c}} \tag{1}$$

where A_0 is the EL intensity at lower frequency, f is the frequency, and A is the EL intensity. The -3 dB cutoff frequency of device A was 1.7- and 1.3-fold compared to the devices B and C, respectively, and the enhancement of response time was caused by the efficient energy transfer in the EML. The maximum -3 dB cutoff frequency of 15.8 MHz was achieved for device A.

4. Conclusion

In conclusion, we investigated fast-response OLEDs with different combination of emitting materials for optical communication applications. By estimating transient characteristics of OLEDs, we found that the large over lap between the PL spectrum of a host material and the absorption spectrum

of a guest material is necessary to improve the response time of OLEDs. In addition, only the rise time of optical response is affected by an emitting material, and less than 100 ns of the rise time was achieved using DSB as a guest material in emitting layer.

References

[1] G. Mauthner, K. Landfester, A. Köck, H. Brückl, M. Kast, C. Stepper, E. J. W. List, Org. Electron. 9 (2008) 164.

[2] H. Kobayashi, S. Kanbe, S. Seki, H. Kigchi, M. Kimura, I. Yudasaka, S. Miyashita, T. Shimada, C. R. Towns, J. H. Burroughes, R. H. Friend, Synth. Met. 111-112 (2000) 125.

[3] S. Lamansky, P. D. Djurovich, D. Murphy, F. Abdel-Razzaq, H. -E. Lee, C. Adachi, P. E. Burrows, S. R. Forrest, M. E. Thompson, J. Am. Chem. Soc. 123 (2001) 4304.

[4] T. Tsutsui, MRS Bulletin 22 (1997) 39.

[5] M. Stößel, J. Steuber, J. Bässing, J. Simmerer, A. Winnacker, H. Neuner, D. Metzdorf, H. -H. Johannes, W. Kowalsky, Synth. Met. 111-112 (2000) 19.

[6] I. D. Parker, J. Appl. Phys. 75 (1994) 1656.

[7] C. W. Tang, S. A. VanSlyke, C. H. Chen, J. Appl. Phys. 65 (1989) 3610.

[8] C. Adachi, R. C. Kwong, P. Djurovich, V. Adamovich, M. A. Baldo, M. E. Thompson, S. R. Forrest, Appl. Phys. Lett. 79 (2001) 2082.

[9] N. K. Patel, S. Cinà, J. H. Burroughes, IEEE Sel. Top. Quantum. Electron. 8 (2002) 346.

[10] Y. Ohmori, K. Hirotake, M. Kaneko, K. Yoshino, M. Ozaki, A. Fujii, M. Hikita, H. Takenaka, T. Taneda, IEEE Sel. Top. Quantum. Electron. 10 (2004) 70.

[11] H. Shimada, J. Yanagi, Y. Matsushita, S. Naka, H. Okada, H. Onnagawa, Jpn. J. Appl. Phys. 45 (2006) 3750.

[12] B. Wei, K. Furukawa, J. Amagai, M. Ichikawa, T. Koyama, Y. Taniguchi, Semicond. Sci. Technol. 19 (2004) L56.

[13] K. Kajii, T. Tsukagawa, T. Taneda, Y. Ohmori, IEICE Trans. Electron. E85-C (2002) 1245.

[14] T. Fukuda, T. Okada, B. Wei, M. Ichikawa, Y. Taniguchi, Appl. Phys. Lett. 90 (2007) 231105.

[15] T. Fukuda, B. Wei, M. Ichikawa, Y. Taniguchi, Jpn. J. Appl. Phys. 46 (2007) 7880.

[16] S. Barth, P. Müller, H. Riel, P. F. Seidler, W. Rieß, H. Vestweber, H. Bässler, J. Appl. Phys. 89 (2001) 3711.

[17] S. W. Culligan, A. C. -A. Chen, J. U. Wallace, K. P. Klubek, C. W. Tang, S. H. Chen, Adv. Func. Mater. 16 (2006) 1481.

[18] T. Fukuda, B. Wei, E. Suto, M. Ichikawa, Y. Taniguchi, Phys. Stat. Sol. RRL 2 (2008) 290.

[19] J. -S. Kim, H. Kajii, Y. Ohmori, Thin Solid Films 499 (2006) 343.

[20] D. Dexter, J. Chem. Phys. 21 (1953) 836.

[21] K. B. Eisenthal, S. Siegel, J. Chem. Phys. 41 (1964) 652.

[22] C. W. Ma, O. Lengyel, J. Kovac, I. Bello, C. S. Lee, S. T. Lee, Chem. Phys. Lett. 397 (2004) 87.

[23] H, Shimada, S. Naka, H.Okada, H. Onnagawa, Jpn. J. Appl. Phys. 44 (2005) 2830.

Figure captions
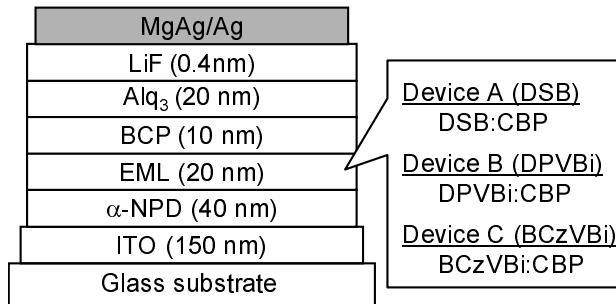
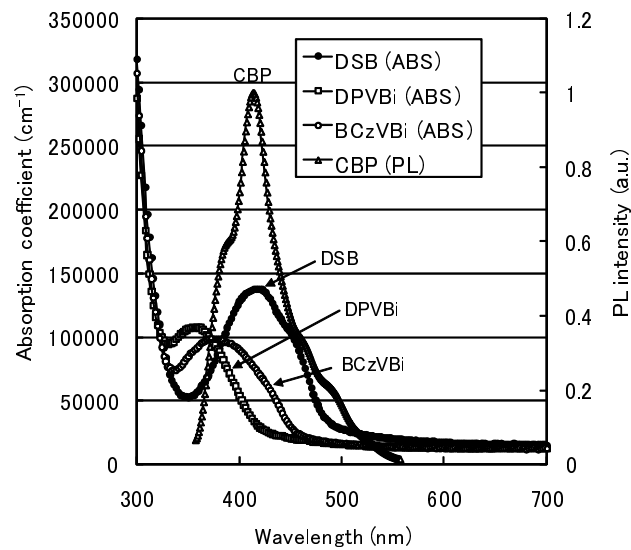Figure 1 Cross sectional view of devices A, B, and C with different guest materials.

Figure 2 Absorption spectra of guest materials (DSB, DPVBi, and BCzVBi) and the PL spectrum of CBP.

Figure 3 (a) Current density-voltage and (b) current efficiency-current density characteristics of devices, of which DSB, DPVBi, and BCzVBi were used as guest materials in the EML, respectively.

Figure 4 (a) rise and (b) decay times of optical responses while applying the pulse voltage with width of 1 μs. The bias voltage was fixed at 6 V.

Figure 5 The frequency dependence of normalized EL intensity for devices A, B, and C. The amplitude of sine wave voltage was 7 V, and the bias voltage was 5 V.

Figure 1: Cross sectional view of devices A, B, and C with different guest materials.
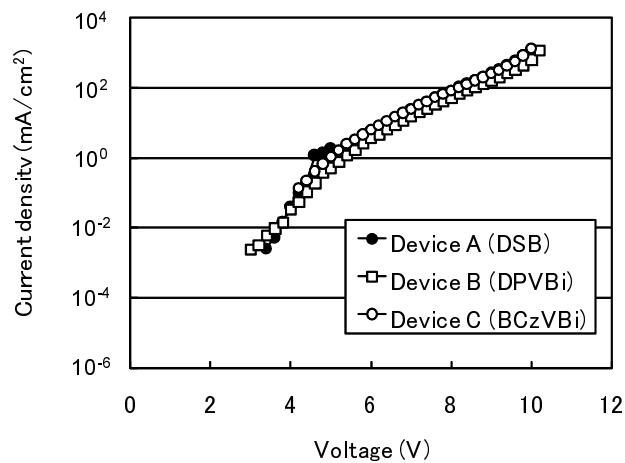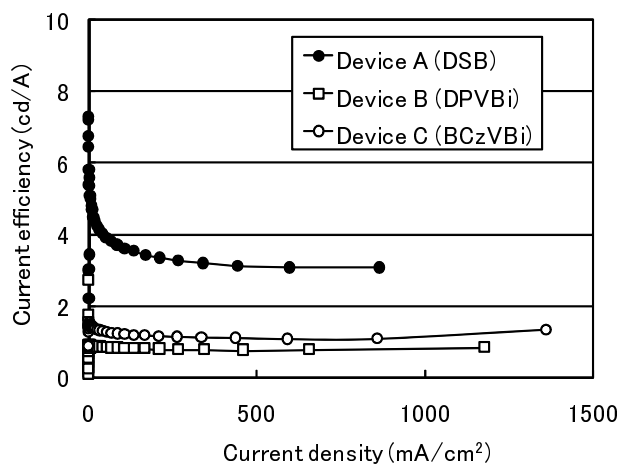

Figure 2: Absorption coefficients of guest materials (DSB, DPVBi, and BCzVBi) and the PL spectrum of CBP.

Figure 3: (a) Current density-voltage and (b) current efficiency-current density character-
istics of devices, of which DSB, DPVBi, and BCzVBi were used as guest materials in the
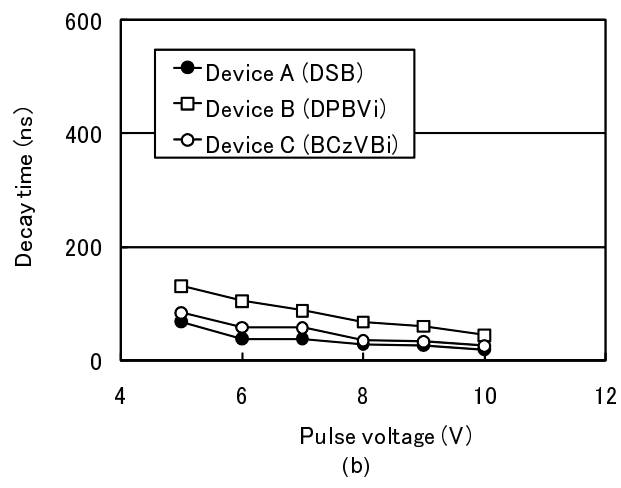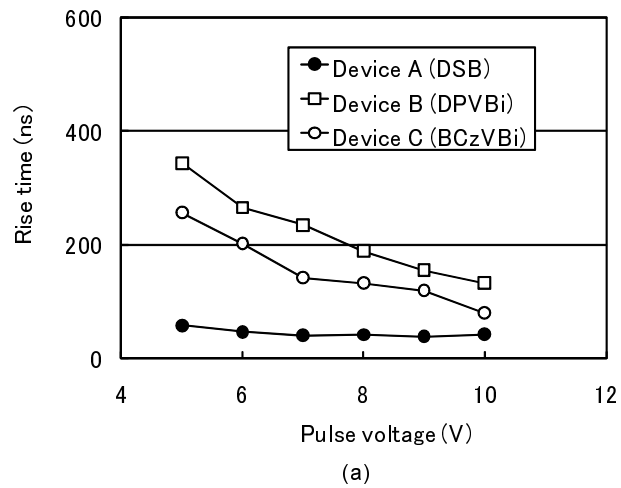EML, respectively.

Figure 4: (a) rise and (b) decay times of optical responses while applying the pulse voltage with width of 1 μs. The bias voltage was fixed at 6 V.
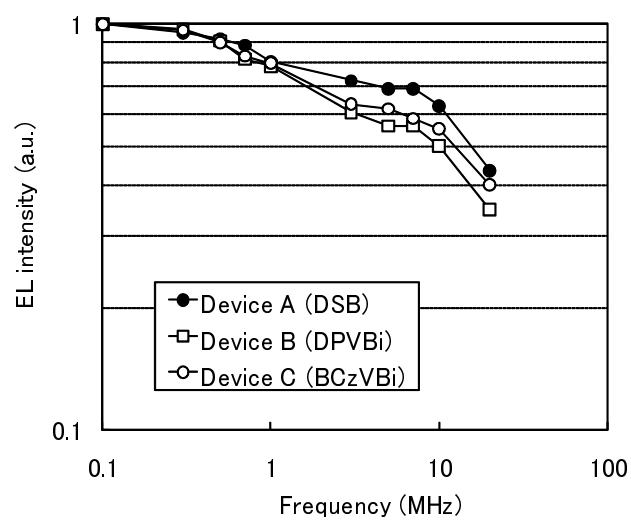
Figure 5: The frequency dependence of normalized EL intensity for devices A, B, and C. The amplitude of sine wave voltage was 7 V, and the bias voltage was 5 V.